Optimization of Phase Map for Simultaneous Dual-frequency MR-based Conductivity Imaging

Saurav ZK Sajib[1], Woo Chul Jeong[1], Hyung Joong Kim[1], Oh In Kwon[2], and Eung Je Woo[1]
[1]*Kyung Hee University, Yongin, Korea,* [2]*Konkuk University, Seoul, Korea*

Target audience

This study might be helpful to the people who are interested in MR-based electrical tissue property mapping such as MREIT and MREPT.

Purpose

In this study, we propose a method to optimize the measured phase signal by finding each weighting factor according to echo signals for MREIT and MREPT using ICNE multi-echo pulse sequence which provides a minimized measured noise.

Methods

We adopt a multiple spin echo pulse sequence based on the ICNE to measure multiple phase data for dual-frequency conductivity imaging.[1] The acquired multiple phase data can be decomposed to the phase term reflecting the magnetic flux density signal induced by the injected current and the other phase term of positive rotating field due to the applied B1 field. We analyse the noise level of the two decomposed phase terms and minimize the measured random noise artifacts by applying optimal combination of multiple phase terms. Also, we apply a denoising technique to both the optimized magnetic flux density of MREIT and the phase signal of MREPT to improve the resolution and sensitivity of the conductivity images.

For evaluation, we built a cylindrical phantom filled with a saline of 0.2 S/m conductivity (Fig. 1). We attached four electrodes on the side of the acrylic container for injecting current. Two different objects were positioned inside phantom. One was a thin hollow cylindrical object with an insulating thin film. We punched four holes which had 2 mm diameter with equally spaced around the circumference. The other was made of an agarose gel to generate different conductivity, spin density and T2-decay comparing to the background saline. The conductivity of agarose gel was 1.10 S/m. It was wrapped in a thin insulating film without holes. A transversal injecting current of 10 mA was introduced into the phantom via a pair of electrodes attached at the middle of the phantom. The imaging parameters were as follows: TR=1200 ms, data acquisition time width Ts = 3.584 ms, echo-spacing=15 ms, matrix size = 128×128, FOV = 180×180 mm^2, slice thickness = 5mm, total number of echo=6, and number of averaging=4. Total imaging time for both vertical and horizontal injection currents was 20 minutes with an interleaved phase encoding acquisition.

Results and Discussion

Figure 2 shows the phase field maps of MREPT (a) and MREIT (b) from all 6 echoes. The images are estimated by properly adding and subtracting the phase signals of the complex data, respectively. Since the electromagnetic wave at the Larmor frequency could penetrate the thin insulating film, the measured phase values for the left object in MREPT could not produce conductivity difference between inside and outside. However, the measured magnetic flux density (B_z) images at the low frequency in MREIT showed the different value inside the left anomaly because MREIT measures the apparent B_z corresponding to the ion mobility and intrinsic conductivities of composite materials.[2] In contrast, the other object of agarose gel cylinder wrapped in the thin insulating film without holes, both two images in Fig. 2(a) and (b) could present distinctions between inside of the object and the background saline. Using the proposed optimization method with the estimated noise standard deviations of measured phase value and B_z, we found the optimal weighting factors for the phase of H^+ and the B_z, respectively. Figure 3 show the determined weighting factors for dual-frequency conductivity images in MREPT (a) and MREIT (b). In MREPT, the intensity of weighting factors was monotonically decreased because the noise levels only depended on T2 decay rate of complex data whereas the weighting factors in MREIT show the different characteristics because they depended on the combination of T2 decay rate and the duration of injected current simultaneously.

Figure 4 show the reconstructed low- (a and b) and high- (c and d) frequency conductivity images using the optimally weighted phase value and B_z without (a and c) and with (b and d) denoising method. Solving the reaction-diffusion equation with the estimated noise standard deviations of phase value and B_z, we effectively reduced the random noise artifacts simultaneously.

Conclusion

We enhanced the dual conductivity images using the optimally weighted magnetic flux density and the phase term of positive-rotating magnetic field based on the analysis of the noise standard deviations and applying the optimization and denoising methods.

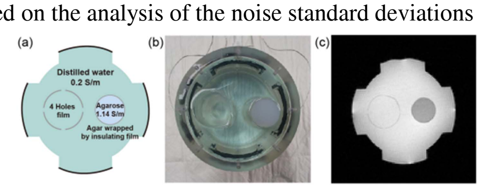

Fig. 1. Experimental setup for phantom imaging. (a) Pantom configuration, (b) top view and (c) MR magnitude images.

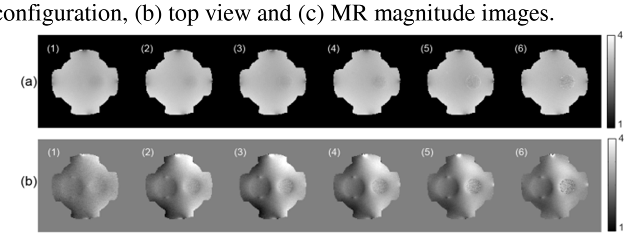

Fig. 2. Phase and magnetic flux density images from six echoes.

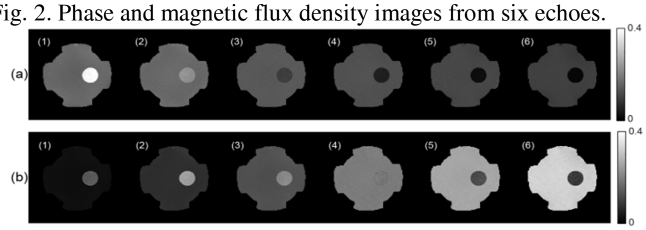

Fig. 3. Calculated weighting factors corresponding to each echoes.

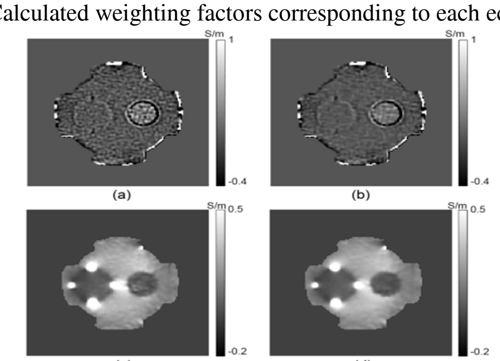

Fig. 4. Optimized simultaneous dual-frequency conductivity images of phantom.

References

1. Minhas AS, Jeong WC, et al. Experimental performance evaluation of multi-echo ICNE pulse sequence in magnetic resonance electrical impedance tomography. Magn. Reson. Med. 2011;66:957-965.
2. Kim HJ, Jeong WC, et al. Simultaneous imaging of dual-frequency electrical conductivity using a combination of MREIT and MREPT. Magn. Reson. Med. in press.